Detecting Foldback Artifacts in Long-reads

Jakob M. Heinz[1,2,3], Matthew Meyerson[3,4,5], Heng Li[1,2,*]

[1]Department of Biomedical Informatics, Harvard Medical School, Boston, MA, United States

[2]Department of Data Science, Dana-Farber Cancer Institute, Boston, MA, United States

[3]Cancer Program, Broad Institute of MIT and Harvard, Cambridge, MA, USA

[4]Department of Medical Oncology, Dana-Farber Cancer Institute, Boston, MA, USA

[5]Department of Genetics, Harvard Medical School, Boston, MA, USA

*Corresponding author: hli@ds.dfci.harvard.edu

Abstract

Long-read sequencing data is useful for detecting large and complex structural variations; however, technical artifacts can lead to false structural variant calls. In our analyses, we became aware of a foldback artifact in long-read data. Therefore, we developed the open-source Breakinator tool to flag putative foldback artifact reads, as well as previously known chimeric artifacts. Through an alignment-based approach, Breakinator can detect artifacts missed by existing quality control tools. We profiled the occurrences of foldbacks and chimeric reads in both nanopore and single-molecule real-time sequences across a range of specimens, library types, sequencing chemistries, sequencing machines, and base-calling software.

Keywords

Long-read sequencing, Nanopore, RNA-Sequencing, Technical artifacts, Quality control

Background

Advances in long-read sequencing technologies, such as those by Pacific Biosciences (PacBio; single-molecule real-time sequencing) and Oxford Nanopore Technologies (ONT; nanopore sequencing), have made the reliable resolution of complex and repetitive regions of the genome possible, which cannot be achieved by short-read sequencing. The ability of long reads to span these complicated regions is useful for detecting large complex structural variations (SV) in the genome [1, 2]. Typically, for long-read SV calling, reads are aligned to a reference genome to identify those with a supplementary alignment, a so-called split read, where a portion of the read maps to one genomic region, and the remainder maps to another distinct region, causing the aligner to split the read into separate alignment blocks [3–5]. However, systemic technical artifacts in the reads can lead to false SV calls. Chimeric reads, technical artifacts that concatenate two distinct sequences, have been a pervasive issue throughout the history of long-read sequencing [6–9]. Technical artifacts can arise through issues in library preparation or computational errors in distinguishing independent molecules [10, 11]

Here, we have become aware of another type of technical artifact, a foldback (also known as a duplicated inversion) [12], where half the read maps to one strand and the other half maps to the same location, but on the opposite strand, appearing as a near-perfect concatemerization of the forward and reverse strands of a read. A previous study by Soneson *et al.* had noted an elevated rate of palindromic reads in ONT direct-cDNA data with supplementary alignments overlapping their primary alignment on the opposite strand. They hypothesized that these may represent un-split reads by the base caller [11]. These foldback artifacts were also noted in the recent somatic SV caller SAVANA by Elrick *et al.*, which includes a preprocessing step to remove putative

44 foldback artifacts from tumors and matched germline controls before collecting SV supporting
45 reads. The authors observed that foldback artifacts typically account for 1–4% of genomic (g)DNA
46 reads that pass their filter across different tumor regions and patients, but could reach as high as
47 20–30% in some cases [13]. While these foldback artifacts have been observed previously, to our
48 knowledge, no studies have performed a systematic characterization of foldback artifacts across
49 library types, sequencing chemistries, and sequencing machines from diverse samples. Therefore,
50 we applied the open-source Breakinator tool we developed to profile foldback and the already
51 well-known chimeric read artifacts in publicly available genomic and transcriptomic datasets,
52 including recent sequencing technologies such as the ONT's latest R10.4 nanopores and PacBio
53 HiFi.

54 Methods

55 All data used in this study were downloaded from publicly available sources, with the links
56 available in Additional file 1. The K562 samples were generated by the SGN-Ex consortium [14].
57 HCC1395 samples were generated by Cotto *et al.* [15]. The mouse tissue samples were generated
58 by Sessegolo *et al.* [16]. The HG002 gDNA samples were downloaded from ONT's 2025 Genome
59 in a Bottle Data (GIAB) Release [17]. The HG002 direct-RNA002, PacBio Iso-seq, and Mas-seq
60 were made available by GIAB. The HG002 dRNA sample SRR30901279 and the HG002 cDNA
61 data were generated by Zheng *et al.*[18] The HG002 PacBio HiFi gDNA is a public dataset made
62 available by PacBio [19]. The PacBio scAAV sample was generated by Talevich *et al*. [20]
63
64 The samples were aligned to their respective reference genomes using Minimap2 [3]. K562
65 and HCC1395 samples were aligned to T2T-CHM13v2.0 [21, 22]. The mouse samples were

aligned to GRCm39 [23]. HG002 samples were aligned to the HG002v1.0.1 diploid genome [24]. To align dRNA ONT, the following parameters were used: "-cx splice -uf -k14 --secondary=no". For ONT direct-cDNA and cDNA alignments, "-cx splice --secondary=no" parameters were used. ONT gDNA data were aligned with "-cx map-ont --secondary=no" parameters. For PacBio Iso-Seq and Mas-Seq data, we used "-cx splice:hq -uf --secondary=no" parameters. Finally, PacBio HiFi data were aligned with "-cx map-pb-- secondary=no." Aligning to a diploid genome decreases the mapping quality of many reads, as there will likely be at least two locations where they map well. To address this issue, HG002 sample reads were aligned to the HG002v1.0.1 diploid genome by aligning the reads to each haplotype separately using Minimap2 with the flags "--secondary=no" and "--paf-no-hit" specified. We wrote a preprocessing script for the Breakinator to compare the alignment of every read to the maternal and paternal haplotype assemblies, choosing to keep the alignment with the highest alignment score. If the alignment scores were equal, then the maternal haplotype alignment was chosen.

The PAF files were generated using either "paftools.js sam2paf -p" on a SAM file or Minimap2 with the "--secondary=no" flag. We designed the Breakinator to parse the input PAF file to detect reads with supplementary alignments. Secondary alignments were ignored. Alignments with mapping quality less than 10 or lengths less than 200 bps were filtered out. The primary and all supplementary alignments for a given read were identified and sorted by read start location. If the first read segment mapped to the forward strand, then the end of the alignment of the first segment and the start of the second segment were identified as the breakpoint location. If the first segment mapped to the reverse strand, the reciprocal start and end locations were taken for the breakpoint. As shown in Fig. 1a, if the breakpoint was to the opposite strand within 200

89 bps of the end of the alignment of the first segment, it was classified as a foldback. If the breakpoint
90 was to another chromosome (interchromosomal) or more than 1 Mb away (intrachromosomal), it
91 was classified as a chimeric read. The 1 Mb default threshold for intrachromosomal chimeras was
92 chosen because only two introns, out of 177,839, on MANE selected protein-coding genes were
93 longer than 1 Mb [25]. If the breakpoint was not chimeric or a foldback, then it was considered a
94 true breakpoint. The identified breakpoints and their classification were generated for every
95 sample. While uncommon, it is possible to have multiple breakpoints on the same read. To classify
96 at the read level, we used the following approach: if there was any foldback or chimeric breakpoint
97 on the read, regardless of how many true breakpoints there were, it was classified as an artifact. If
98 there were multiple foldback or chimeric breakpoints on the read, the read was classified according
99 to which breakpoint occurred most frequently. If they were equal, then the read was classified as
100 chimeric. All summary statistics are generated using the read level classifications.
101
102 To compare how existing tools detect the reads we had identified as artifactual, we filtered
103 all reads with fastplong, porechop, and restrander, respectively [26–28]. Fastplong was run with
104 the following command: "fastplong -i sample.fastq -o filter_pass.fastq --failed_out
105 failed_reads.fastq." Restrander was run only on our cDNA samples, as it didn't support any other
106 data types, with the command "restrander sample.fastq filter_pass.fastq config.json." Restrander
107 required a configuration file of adaptor sequences, so for samples that did not have their library
108 version supported by Restrander, we ran them with the closest version of the library supported by
109 Restrander. For example, DCS108 samples were run with the SQK-DCS109 config file. Porechop
110 was also only run on the transcriptomic data using the command: "porechop -i sample.fastq --
111 discard_middle -o filter_pass.fastq." For each tool, the read IDs that passed their respective filter

112 were used to subset the reads we found to pass our default filter of a minimum of 200 bps of
113 alignment and a mapping quality of at least 10. The reads classified as foldback, chimeric, or any
114 breakpoint were similarly subset to include only the reads that passed the respective filter to
115 calculate the proportions reported in Additional file 2. PyChopper [29] was only run on the three
116 HCC1395 samples, as we found it to be too slow to run on all samples. The length of the unaligned
117 sequence between aligning segments of the breakpoint was identified by running the Breakinator
118 with the "--rcoord" flag to output the read coordinates of the breakpoint along with the reference
119 coordinates of the breakpoint. The reads were subset to foldback, chimeric, and true breakpoints,
120 and the proportions of reads with at least 11 bps between the read coordinates of the breakpoint
121 were calculated for each subset in Additional file 3.
122
123 To generate summary statistics for Fig.2, the Breakinator was run on every sample using
124 the "-i in.paf --tabular -o out.txt" parameters. The PacBio scAAV sample was evaluated with the
125 Breakinator using the stricter parameters of a symmetry filter and half the default margin (--sym -
126 -margin 0.025). To determine which breakpoints were recurrent, we extracted the subset of
127 breakpoints that were flagged as either "Foldback", "Chimeric", or "True Break", respectively,
128 then for each file we merged any breakpoints that were within 100 bps of each other to account for
129 inexact alignments around the breakpoint, to determine the number of reads supporting a
130 breakpoint using our merge_breaks.py script. The merging process was run with the -s flag set to
131 2, 5, and 10, which sets the minimum number of reads needed to support a breakpoint. The reads
132 that had support of other reads at the respective support thresholds were summed and divided by
133 the total number of reads in the subset to determine the proportion of reads with support, as shown
134 in Fig. 2d.

The SGNEx K562 direct-cDNA replicate 2 run 1 sample was chosen to investigate the raw electrical signal that the ONT base caller interprets because its fast5 files were publicly available, and we discovered numerous putative artifacts in the reads. The fast5 files were indexed with nanopolish using "nanopolish index -d fast5_directory reads.fastq" [30]. Nanopolish eventalign was used to determine which region of the raw signal corresponds to the breakpoint location in the read. To explore the signal in read coordinates, we converted the read fastq file to a fasta file to use as the genome input, then aligned the reads to themselves with "minimap2 -ax map-ont -o reads2reads.sam reads.fastq reads.fa " and used this as the BAM input for the eventalign command as follows: "nanopolish eventalign -r reads.fastq -b reads2reads.bam -g reads.fasta --signal-index". We chose eight reads in total to investigate the raw signal. We investigated foldbacks, chimeras, and true breakpoints with and without unaligned sequences in the middle, as well as a read with no breakpoint. The start and end of the breakpoint locations in the read were determined from the Breakinator output and converted to the signal coordinates using the nanopolish eventalign output. The fast5 samples were graphed, and the breakpoint coordinates in the signal were highlighted to manually investigate the signal for any signs of increased noise around the breakpoint.

Results

The Breakinator tool identifies putative foldback and chimeric artifacts by parsing a read alignment file. Our tool extracts the primary and all supplemental alignments of a read and classifies them as either a true breakpoint, chimeric, or foldback using the classification scheme in Fig. 1a. While all metrics can be set by the user, we classify a chimeric artifact as a read that has segments mapping to different chromosomes, or more than 1 Mb apart within the same

chromosome. We classify a read as a foldback artifact if the supplementary alignment maps to the same location as the primary alignment (within 200 bps) on the opposite strand. For samples where true foldback events may be expected, as in cancers, we added a symmetry option to our tool to only report reads as foldback artifacts if the foldback occurs within a 5% margin on either side of the middle of the read, to retain true foldback event supporting reads.

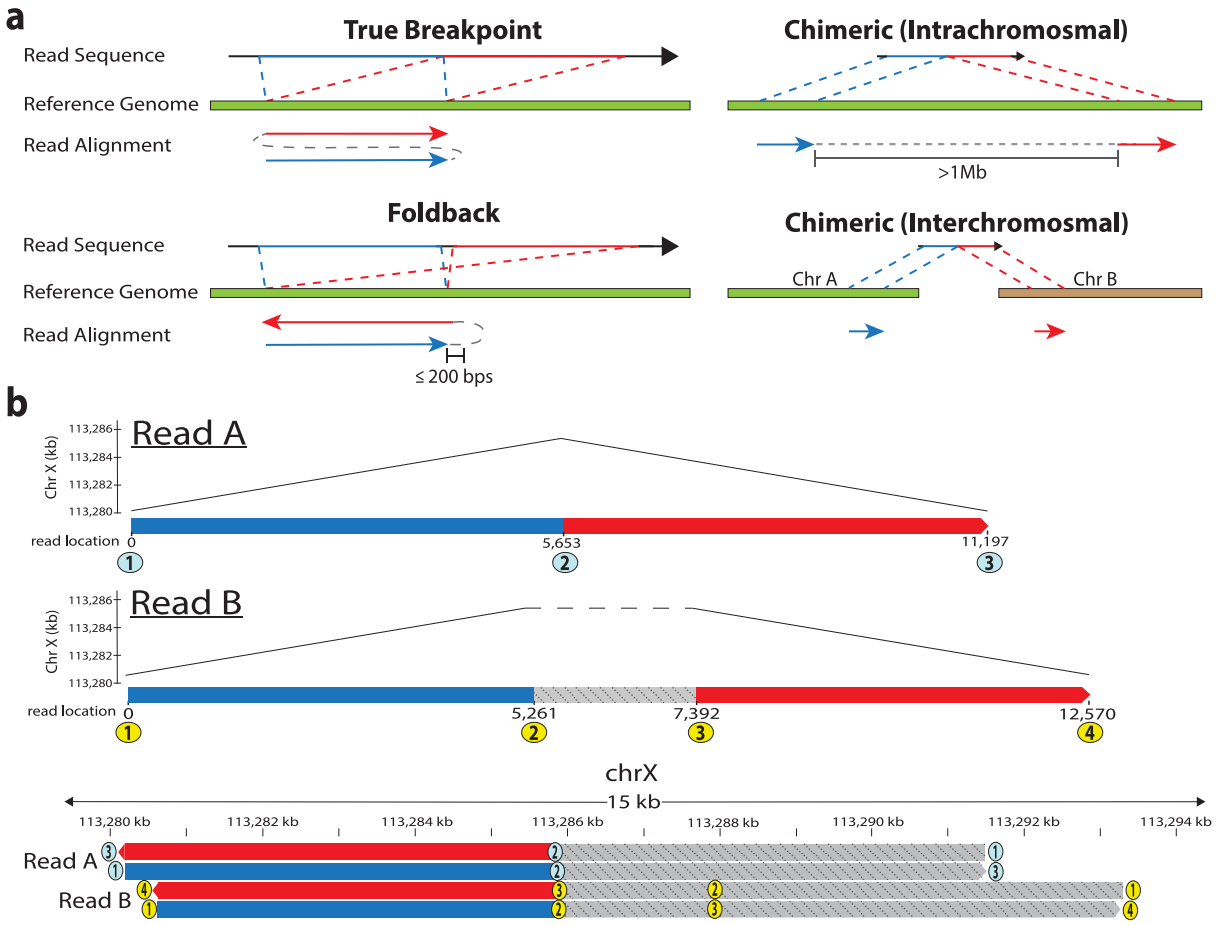

Fig. 1 a). Metrics used to define types of breakpoints observed in this study. A "True Break" is a breakpoint that is not found to be chimeric or a foldback, such as the tandem duplication example shown here. A "Foldback" is a read where the second segment maps to approximately the same location (within 200bps) as the first segment, but on the opposite strand. A "Chimeric" is where the second segment maps more than 1 Mb away on the same chromosome (intrachromosomal) or

168 to a different chromosome (interchromosomal). b) IGV schematization of two foldback artifact
169 reads from the HG002_PAW70337_sup sample supporting the same breakpoint at approximately
170 113,286 kb on chromosome X of the HG002 diploid assembly. Read A (5f80430c-2b83-408b-
171 89b2-63b61b1173cc) is an example of a read with no sequence between the two segments of the
172 foldback. Read B (115c006d-16a6-47b1-bf5c-c5eb9bb85f69) is an example where there are ~2kb
173 of sequence between the segments.
174
175 To verify that our tool properly identifies foldback events, we used PacBio's samples of
176 self-complementary adeno-associated viruses (scAAV) CBA-eGFP as a positive control. Since
177 scAAV-CBA-eGFP constructs were designed to be perfectly palindromic, we expected our tool to
178 detect them as foldbacks. With the Breakinator, we find that 97.49% CBA-eGFP sample reads are
179 scAAV compared to the 97.69% reported by Talevich *et al*. [20]. This verification also presented
180 an interesting additional use case for the Breakinator for the rapid identification of scAAVs in a
181 sample.
182
183 We first noticed a potential technical artifact when analyzing transcriptomic data of the
184 HCC1395 cell line generated by Cotto *et al.* [15]. In the ONT direct-cDNA samples, we observed
185 many reads with supplementary alignments overlapping the primary alignment on the opposite
186 strand, indicative of a foldback SV, that were not present in the ONT direct-RNA sample run on
187 the same RNA replicate. Manual inspection of the unique breakpoint locations in IGV [31] found
188 that those detected from direct-RNA had supporting evidence from PacBio HiFi gDNA sequences,
189 while most of the direct-cDNA breakpoints did not, leading us to suspect that many of these events
190 were caused by a technical artifact. After developing the Breakinator, we used it to identify all

191 breakpoints in the sample and merge breakpoints in the same region (see Methods). We found
192 35,843 unique breakpoint locations with at least five supporting reads in the direct-cDNA samples,
193 compared to just eight in the direct-RNA. While foldback SVs occur in cancer genomes, they have
194 not been observed at such a high frequency [12], and are not expected to vary so greatly by library
195 type.
196
197 To explore whether this was a dataset-specific sequencing result or a systemic technical
198 artifact, we downloaded publicly available datasets representing four library types: direct-RNA,
199 direct-cDNA, cDNA, and gDNA, from four sample types (HG002 cell line, K562 cell line,
200 HCC1395 cell line, and mouse tissue). A range of sequencing chemistries, machines, and base-
201 calling software were evaluated through these samples (Additional file 1). The HG002 samples
202 offer a useful neutral background to investigate technical artifacts because they have a high-quality
203 personal diploid reference assembly to which the reads can be aligned [24]. Therefore, we would
204 expect no germline variants, given that this is the reference, only variations between samples of
205 the cell line, which are likely limited [32]. Each sample was aligned to the corresponding reference
206 genome with the appropriate Minimap2 [3] parameters for each data type (see Methods). Fig. 1b
207 demonstrates two-foldback reads identified by the Breakinator. The reads are both nearly perfectly
208 palindromic and map to the same breakpoint location, yet Read A has no sequence between
209 mappings, while Read B has ~2kb of sequence that could be searched for retained adaptors. 27
210 other reads (not shown) cover this foldback location, with no indication of a breakpoint.
211 Commonly used quality control tools for long reads, such as fastplong, Porechop, pychopper, and
212 Restrander [26–29], did not identify many of the foldback or chimeric reads flagged by the
213 Breakinator (Additional file 2). We found that typically fewer than half of the putative artifactual

214 reads we detected had more than 11 bps of non-mapping sequence between alignments (Additional
215 file 3), making it unlikely that existing tools could detect retained adapter sequences in these reads.
216
217 Summary statistics across library types and samples evaluated with the Breakinator are
218 shown in Fig. 2a. ONT direct-cDNA samples were found to have substantially elevated levels of
219 foldback artifacts (~10-25% of all reads). Meanwhile, at most one foldback read was observed in
220 each of the ONT direct-RNA samples. The ONT cDNA samples had the lowest rates of foldback
221 artifacts (~0.1 – 0.2%). In ONT gDNA, we observed foldback rates of ~0.5–0.7%. While only
222 three PacBio samples were investigated, they did not show any evidence of systemic foldback
223 artifacts. There were virtually no foldback reads observed in the PacBio HiFi (Revio) or Mas-Seq
224 (Vega) data, while 0.04% of the Iso-Seq (Sequel II) reads were considered foldbacks. For five of
225 the samples, from K562 and HCC1395 cells, the same RNA replicate was sequenced with different
226 technologies, allowing for direct comparisons in the rates of foldbacks and chimeras across
227 libraries without replicate bias. It was observed that for all replicates, the rates of foldbacks and
228 chimeras were much higher in ONT direct-cDNA library samples than in other libraries, as shown
229 in Fig. 2b.

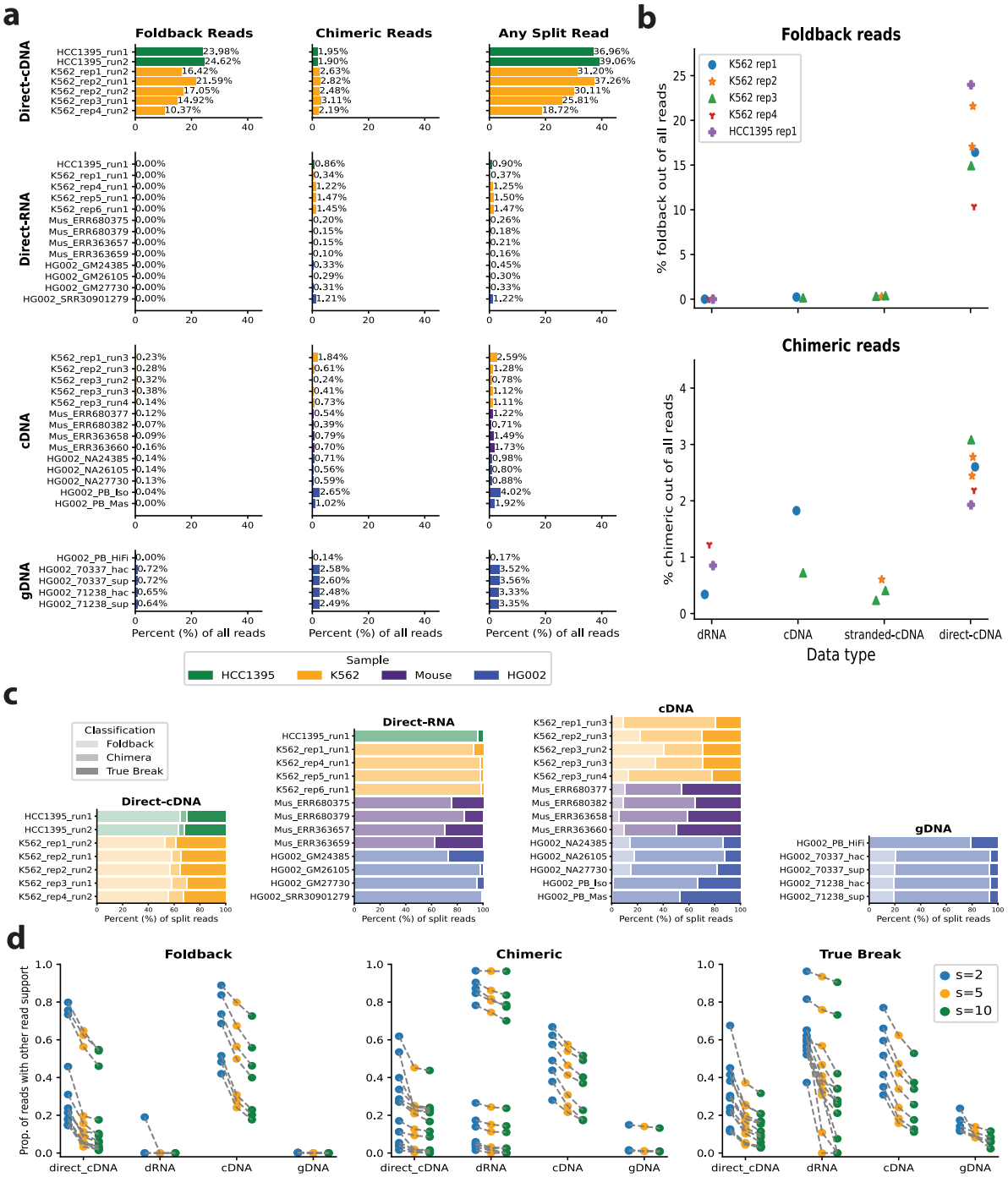

Fig. 2. a) The observed rates of Foldback, Chimeric, and any split read out of all reads that passed the filtering criteria for direct-cDNA, direct-RNA, cDNA, and gDNA data from four different sample types: HCC1395, K562, mouse tissue, and HG002. B) Paired comparisons for the five RNA replicates that were sequenced with different technologies for both foldback and chimeric

reads. c) The proportion of Foldback, Chimeric, and True Break reads in relation to the number of split reads. d) Recurrence of breakpoints at 2, 5, and 10 supporting reads for Foldback, Chimeric, and True Break reads.

To explore the potential effects of these artifactual reads in SV calling, we investigated the proportion of reads used for SV calling, namely, reads with split alignments, that they represent. In cDNA, foldback artifacts account for 10-20% of all split reads, while chimeras are ~30-40%. In gDNA, foldbacks are also 15-20% of split reads, and chimeric reads are 50-60% of all split reads (Fig. 2.c). These artifactual reads were also observed to be recurrent at the same locations, which made it more likely they would be called as a false positive SV. Fig. 2d highlights that many of the locations to which these reads align have more than 2, 5, or 10 reads of support. Finally, we investigated the raw signal of eight putative artifactual reads from the SG-NEx K562 direct-cDNA replicate 2 run 1 to visualize the electrical signal interpreted by the base-caller. We did not observe any notable difference in signal around the breakpoint region for artifacts compared to true breakpoints (Additional file 4).

Discussion

In this study, we documented the rate of foldback artifacts in long-read sequencing data across a diverse set of samples. In addition, we developed the open-source Breakinator tool to report putative foldback artifacts as well as the already well-profiled chimeric artifacts in long-read data. While an alignment-based artifact detection method, as is implemented by the Breakinator, may lead to issues in distinguishing true SV reads from artifact reads and introduce reference bias, the increased specificity offered by alignment to a reference can be useful; This is evidenced by our ability to detect foldback artifact reads that are missed by commonly used

259 quality control tools such as fastplong, Porechop, Restrander, and pychopper [26–29]. We
260 suspect these artifacts are missed due to the tools' reliance on identifying adapter sequences
261 within the middle of a read sequence to identify a concatemerized read. We find that less than
262 half of the putative artifactual reads identified by the Breakinator have any searchable sequence
263 between alignments of the read segments (Fig. 1b). Various assemblers, such as Canu, Flye, and
264 MECAT, use the alignments of reads to each other or assembled contigs to detect technical
265 artifacts [33–35]. This approach is free of reference bias and does not rely on adaptor sequence
266 matches, yet it is very computationally expensive and does not scale well to a quality control tool
267 that would not otherwise perform these alignments.
268
269 While the rates of putative foldback and chimeric artifacts across all reads are relatively
270 low for libraries other than ONT direct-cDNA (Fig. 2a), they represent a far larger proportion of
271 the split alignment reads used for SV calling. Fig. 2c highlights that these artifacts can cause
272 issues even with ONT gDNA or cDNA, in which foldback artifacts represent at most 0.72% of
273 all reads, yet represent approximately 20% of the split reads used for SV calling. We suspect the
274 rate of foldback artifacts is lowest in the cDNA samples, as cDNA is the only library type in this
275 study that undergoes PCR amplification, and palindromic sequences such as these foldbacks are
276 known to be difficult to PCR amplify, as they will bind to themselves [36, 37].
277
278 Given that the rates of foldback artifacts appear relatively consistent among sequencing
279 runs of the same data type, but vary between data types that are prepared with different
280 chemistries, we believe it is most likely that these artifacts arise during library preparation, rather
281 than a failure of the base-caller to recognize a pore-open signal or an adapter sequence, as was

hypothesized by Soneson *et al*. [11]. Additionally, we observed both forward and reverse strands of foldback and chimeric reads, which can only arise during library preparation, compared to an informatic chimera, which would only occur in one reading direction. Lastly, our analysis of a subset of ONT raw electrical signals did not reveal any noise around putative breakpoints, indicating that the foldback artifact molecules likely passed smoothly through the pore.

Conclusions

We present evidence of a new technical artifact, a foldback read. If these technical artifacts are not properly removed, they can lead to tangles in an assembly graph or false-positive SV calls. We developed the open-source Breakinator tool to flag putative foldback and chimeric technical artifacts in long-read sequences. Many current quality control tools rely on detecting incorrectly incorporated adapter sequences, but through a reference alignment-based approach, we can detect reads that may not have retained non-sample sequence, but still likely represent a non-real biological concatenation. In this study, we profiled both ONT and PacBio data across a range of specimens, library types, sequencing chemistries, sequencing machines, and base-callers. We find that foldback artifacts occur throughout ONT library types and are particularly high in direct-cDNA libraries. We believe the Breakinator will offer a useful tool for quality control in long-read sequencing analyses, particularly for SV calling.

Declarations

Ethics approval and consent to participate

Not applicable.

Consent for publication

Not applicable.

Additional files

Additional_file_1.xlsx – All public data used in this study and their sources. Includes metadata on datatype, sequencer, pore, chemistry, and base-caller.

Additional_file_2.xlsx – Proportions of reads remaining, including artifact subsets, after filtering with other current tools (fastplong, Porechop, pychopper, and Restrander).

Additional_file_3.xlsx – Proportions of reads that had 11 bps or greater of unmapped read sequence between alignment blocks.

Additional_file_4.html – SGNEx K562 direct-cDNA replicate 2 run 1 raw signal analysis around identified breakpoints for eight reads.

Availability of data and materials

The Breakinator tool and additional software are available on GitHub at https://github.com/jheinz27/breakinator. All data used in this study were previously made publicly available, and their sources are listed in Additional file 1. The alignment files for every sample, as well as all breakpoints identified and their Breakinator classification, are available on Zenodo at: https://zenodo.org/records/15882143.

Competing interests

M.M. holds equity in Bayer, Delve Bio, Isabl, and Karyoverse; consults for Delve Bio; receives research funding from Bayer; and receives patent licensing payments from Bayer and Labcorp.

Funding

J.M.H. is supported by the U.S. National Institutes of Health training grant T32HG002295. M.M. is supported by NIH grants R35CA197568 and U24CA264029. H.L. is supported by NIH grants U24CA294203 and R01HG010040

Authors' contributions

J.M.H., M.M., and H.L conceived the project. J.M.H. implemented the method, analyzed the data, and drafted the manuscript. M.M. and H.L provided edits. All authors read and approved the final manuscript.

Acknowledgments

We would like to thank Drs. Neng Huang, Owen Hirschi, Alaina Shumate, Maximillian Marin, Victoria Popic, and Kar-Tong Tan, as well as all members of the Meyerson and Li labs, for their helpful discussions.

References

1. Mahmoud M, Gobet N, Cruz-Dávalos DI, Mounier N, Dessimoz C, Sedlazeck FJ. Structural variant calling: the long and the short of it. Genome Biol. 2019;20. https://doi.org/10.1186/s13059-019-1828-7.
2. Sedlazeck FJ, Rescheneder P, Smolka M, Fang H, Nattestad M, Von Haeseler A, et al. Accurate detection of complex structural variations using single-molecule sequencing. Nature Methods 2018 15:6. 2018;15:461–8. https://doi.org/10.1038/s41592-018-0001-7.
3. Li H. Minimap2: pairwise alignment for nucleotide sequences. Bioinformatics. 2018;34:3094–100. https://doi.org/10.1093/BIOINFORMATICS/BTY191.
4. Smolka M, Paulin LF, Grochowski CM, Horner DW, Mahmoud M, Behera S, et al. Detection of mosaic and population-level structural variants with Sniffles2. Nature Biotechnology 2024 42:10. 2024;42:1571–80. https://doi.org/10.1038/s41587-023-02024-y.

5. Keskus A, Bryant A, Ahmad T, Yoo B, Aganezov S, Goretsky A, et al. Severus: accurate detection and characterization of somatic structural variation in tumor genomes using long reads. medRxiv. 2024;:2024.03.22.24304756. https://doi.org/10.1101/2024.03.22.24304756.

6. Buck D, Weirather JL, de Cesare M, Wang Y, Piazza P, Sebastiano V, et al. Comprehensive comparison of Pacific Biosciences and Oxford Nanopore Technologies and their applications to transcriptome analysis. F1000Res. 2017;6:100. https://doi.org/10.12688/F1000RESEARCH.10571.2.

7. Eccles D, White R, Pellefigues C, Ronchese F, Lamiable O. Investigation of chimeric reads using the MinION. F1000Res. 2017;6:631. https://doi.org/10.12688/F1000RESEARCH.11547.2.

8. Yang C, Lo T, Nip KM, Hafezqorani S, Warren RL, Birol I. Characterization and simulation of metagenomic nanopore sequencing data with Meta-NanoSim. Gigascience. 2022;12:1–11. https://doi.org/10.1093/GIGASCIENCE/GIAD013.

9. Stock W, Rousseau C, Dierickx G, D'hondt S, Amadei Martínez L, Dittami SM, et al. Breaking free from references: a consensus-based approach for community profiling with long amplicon nanopore data. Brief Bioinform. 2024;26. https://doi.org/10.1093/BIB/BBAE642.

10. Li Y, Wang T-Y, Guo Q, Ren Y, Lu X, Cao Q, et al. A Genomic Language Model for Chimera Artifact Detection in Nanopore Direct RNA Sequencing. bioRxiv. 2024;:2024.10.23.619929. https://doi.org/10.1101/2024.10.23.619929.

11. Soneson C, Yao Y, Bratus-Neuenschwander A, Patrignani A, Robinson MD, Hussain S. A comprehensive examination of Nanopore native RNA sequencing for characterization of complex transcriptomes. Nature Communications 2019 10:1. 2019;10:1–14. https://doi.org/10.1038/s41467-019-11272-z.

12. Li Y, Roberts ND, Wala JA, Shapira O, Schumacher SE, Kumar K, et al. Patterns of somatic structural variation in human cancer genomes. Nature 2020 578:7793. 2020;578:112–21. https://doi.org/10.1038/s41586-019-1913-9.

13. Elrick H, Sauer CM, Espejo Valle-Inclan J, Trevers K, Tanguy M, Zumalave S, et al. SAVANA: reliable analysis of somatic structural variants and copy number aberrations using long-read sequencing. Nat Methods. 2025;22:1436–46. https://doi.org/10.1038/S41592-025-02708-0;SUBJMETA=2056,208,211,308,631,67,69,692;KWRD=CANCER+GENOMICS,GENETICS+RESEARCH,GENOMIC+INSTABILITY.

14. Chen Y, Davidson NM, Wan YK, Yao F, Su Y, Gamaarachchi H, et al. A systematic benchmark of Nanopore long-read RNA sequencing for transcript-level analysis in human cell lines. Nature Methods 2025 22:4. 2025;22:801–12. https://doi.org/10.1038/s41592-025-02623-4.

15. Cotto KC, Feng YY, Ramu A, Richters M, Freshour SL, Skidmore ZL, et al. Integrated analysis of genomic and transcriptomic data for the discovery of splice-associated variants in cancer. Nature Communications 2023 14:1. 2023;14:1–18. https://doi.org/10.1038/s41467-023-37266-6.

16. Sessegolo C, Cruaud C, Da Silva C, Cologne A, Dubarry M, Derrien T, et al. Transcriptome profiling of mouse samples using nanopore sequencing of cDNA and RNA molecules. Sci Rep.

2019;9:1–12. https://doi.org/10.1038/S41598-019-51470-9;TECHMETA=38,45,91;SUBJMETA=114,1949,514,61,631;KWRD=COMPUTATIONAL+BIOLOGY+AND+BIOINFORMATICS,RNA+SEQUENCING.

17. Genome in a Bottle Data Release 2025.01 | EPI2ME Blog. https://epi2me.nanoporetech.com/giab-2025.01/. Accessed 11 Jun 2025.

18. Zheng Z, Yu X, Chen L, Lee Y-L, Xin C, On A, et al. Clair3-RNA: A deep learning-based small variant caller for long-read RNA sequencing data. https://doi.org/10.1101/2024.11.17.624050.

19. Datasets - PacBio - Highly accurate long-read sequencing. https://www.pacb.com/connect/datasets/. Accessed 11 Jun 2025.

20. Talevich E, Tseng E, Diallo A, Sellami N, Elliott A, Cantarel BL, et al. Standardized Nomenclature and Reporting for PacBio HiFi Sequencing and Analysis of rAAV Gene Therapy Vectors. bioRxiv. 2024;:2024.05.07.592296. https://doi.org/10.1101/2024.05.07.592296.

21. Nurk S, Koren S, Rhie A, Rautiainen M, Bzikadze A V., Mikheenko A, et al. The complete sequence of a human genome. Science (1979). 2022;376:44–53. https://doi.org/10.1126/SCIENCE.ABJ6987/SUPPL_FILE/SCIENCE.ABJ6987_MDAR_REPRODUCIBILITY_CHECKLIST.PDF.

22. Rhie A, Nurk S, Cechova M, Hoyt SJ, Taylor DJ, Altemose N, et al. The complete sequence of a human Y chromosome. Nature 2023 621:7978. 2023;621:344–54. https://doi.org/10.1038/s41586-023-06457-y.

23. Waterston RH, Lindblad-Toh K, Birney E, Rogers J, Abril JF, Agarwal P, et al. Initial sequencing and comparative analysis of the mouse genome. Nature. 2002;420:520–62. https://doi.org/10.1038/NATURE01262,.

24. Rautiainen M, Nurk S, Walenz BP, Logsdon GA, Porubsky D, Rhie A, et al. Telomere-to-telomere assembly of diploid chromosomes with Verkko. Nat Biotechnol. 2023;41:1474–82. https://doi.org/10.1038/S41587-023-01662-6;SUBJMETA=114,1948,208,2302,2785,514,631,728;KWRD=DNA+SEQUENCING,GENOME+ASSEMBLY+ALGORITHMS,HAPLOTYPES.

25. Morales J, Pujar S, Loveland JE, Astashyn A, Bennett R, Berry A, et al. A joint NCBI and EMBL-EBI transcript set for clinical genomics and research. Nature 2022 604:7905. 2022;604:310–5. https://doi.org/10.1038/s41586-022-04558-8.

26. Chen S. Ultrafast one-pass FASTQ data preprocessing, quality control, and deduplication using fastp. iMeta. 2023;2:e107. https://doi.org/10.1002/IMT2.107;JOURNAL:JOURNAL:2770596X.

27. rrwick/Porechop: adapter trimmer for Oxford Nanopore reads. https://github.com/rrwick/Porechop. Accessed 18 May 2025.

28. Schuster J, Ritchie ME, Gouil Q. Restrander: rapid orientation and artefact removal for long-read cDNA data. NAR Genom Bioinform. 2023;5:lqad108. https://doi.org/10.1093/NARGAB/LQAD108.

29. epi2me-labs/pychopper: cDNA read preprocessing. https://github.com/epi2me-labs/pychopper. Accessed 17 May 2025.
30. Loman NJ, Quick J, Simpson JT. A complete bacterial genome assembled de novo using only nanopore sequencing data. Nature Methods 2015 12:8. 2015;12:733–5. https://doi.org/10.1038/nmeth.3444.
31. Robinson JT, Thorvaldsdóttir H, Winckler W, Guttman M, Lander ES, Getz G, et al. Integrative Genomics Viewer. Nat Biotechnol. 2011;29:24. https://doi.org/10.1038/NBT.1754.
32. Liu Y, Mi Y, Mueller T, Kreibich S, Williams EG, Van Drogen A, et al. Multi-omic measurements of heterogeneity in HeLa cells across laboratories. Nat Biotechnol. 2019;37:314–22. https://doi.org/10.1038/S41587-019-0037-Y;SUBJMETA=1647,2067,553,631,80;KWRD=CELL+BIOLOGY,PROTEOMIC+ANALYSIS,SYSTEMS+BIOLOGY.
33. Koren S, Walenz BP, Berlin K, Miller JR, Bergman NH, Phillippy AM. Canu: Scalable and accurate long-read assembly via adaptive κ-mer weighting and repeat separation. Genome Res. 2017;27:722–36. https://doi.org/10.1101/GR.215087.116/-/DC1.
34. Kolmogorov M, Yuan J, Lin Y, Pevzner PA. Assembly of long, error-prone reads using repeat graphs. Nat Biotechnol. 2019;37:540–6. https://doi.org/10.1038/S41587-019-0072-8;SUBJMETA.
35. Xiao C Le, Chen Y, Xie SQ, Chen KN, Wang Y, Han Y, et al. MECAT: Fast mapping, error correction, and de novo assembly for single-molecule sequencing reads. Nat Methods. 2017;14:1072–4. https://doi.org/10.1038/NMETH.4432;TECHMETA.
36. Devine SE, Chissoe SL, Eby Y, Wilson RK, Boeke JD. A Transposon-Based Strategy for Sequencing Repetitive DNA in Eukaryotic Genomes. Genome Res. 1997;7:551–63. https://doi.org/10.1101/GR.7.5.551.
37. Tanaka H, Tapscott SJ, Trask BJ, Yao MC. Short inverted repeats initiate gene amplification through the formation of a large DNA palindrome in mammalian cells. Proc Natl Acad Sci U S A. 2002;99:8772–7. https://doi.org/10.1073/PNAS.132275999/ASSET/DEEE332B-28CA-4935-9282-FE466CDECD9C/ASSETS/GRAPHIC/PQ1322759005.JPEG.